JCTC Journal of Chemical Theory and Computation

Density-Fitting Method in Symmetry-Adapted Perturbation Theory Based on Kohn−Sham Description of Monomers

Rafał Podeszwa,* Robert Bukowski, and Krzysztof Szalewicz

Department of Physics and Astronomy, University of Delaware, Newark, Delaware 19716

Received December 2, 2005

Abstract: We present a new implementation of symmetry-adapted perturbation theory of intermolecular interactions based on Kohn−Sham description of monomers. With density-fitting of molecular integrals, the scaling of the computational cost of the method is reduced from the sixth to the fifth power of the system size. Computational requirements of some operations scaling as the fifth power have also been significantly reduced. The new method allows an accurate treatment of molecules consisting of as many as a few dozen of atoms, using both nonhybrid and hybrid density functionals.

I. Introduction

Structure and properties of various atomic and molecular systems, from clusters to condensed phases to biological molecules, are determined by weak intermolecular interactions, also referred to as van der Waals interactions. These effects have been successfully studied ab initio, both within the supermolecular framework, using the coupled-cluster method and many-body perturbation theory, and perturbatively in intermolecular interaction operator V, using methods such as symmetry-adapted perturbation theory (SAPT).[1−3] Unfortunately, the computational cost of the wave function-based approaches increases prohibitively fast with system size N, as $O(N^7)$ for methods including triple excitations. Density functional theory (DFT) is much less time-consuming; however, the existing versions of DFT, when applied within the supermolecular approach, fail to reproduce the dispersion interaction, an important part of the van der Waals force. This problem is due to the fact that dispersion forces result from long-range correlations between electrons, whereas the current exchange-correlation potentials model only local correlation effects.

Another approach to the calculations of interaction energies is based on SAPT but utilizes the description of the interacting monomers in terms of Kohn−Sham (KS) orbitals and orbital energies, a method now called SAPT(KS). The predictions of the original version of this approach, proposed by Williams and Chabalowski,[4] were rather poor, and these authors conjectured that the reason could be the wrong asymptotic behavior of the KS electron densities. In a subsequent development, Misquitta and one of the present authors[5] and independently Hesselmann and Jansen[6,7] have shown that indeed if the asymptotic behavior is corrected, the accuracy of the electrostatic, exchange, and induction terms greatly improves. Only the dispersion component was still inaccurate. This problem was found[8,9] to be due to the use of a formula asymptotically related to uncoupled dynamic polarizabilities. When, instead, the dispersion energies were calculated from frequency-dependent density susceptibility (FDDS) functions, also referred to as propagators, obtained from the time-dependent DFT (TD-DFT) theory at the coupled Kohn−Sham (CKS) level, the results became very accurate. The SAPT approach based on asymptotically corrected KS calculations and on CKS FDDS's was proposed in ref 10 and referred to as SAPT(DFT). The method can be shown to be potentially exact for all major components of the interaction energy (asymptotically for exchange interactions) in the sense that these components would be exact if the DFT description of the monomers were exact.[5,8,11] Applications to a number of small dimers have shown that SAPT(DFT) provides surprisingly accurate individual interaction components, often more accurate than the standard SAPT at the currently programmed level.[10,11] Applications to larger dimers were presented in refs 12 and 13.

10.1021/ct050304h CCC: $33.50
Published on Web 02/18/2006

The nominal scaling of SAPT(KS) is $O(N^5)$ and that of SAPT(DFT) is $O(N^6)$, in both cases significantly better than the $O(N^7)$ scaling of the regular SAPT. Despite this better scaling, it was not feasible to apply SAPT(DFT) to very large systems, e.g., the ones of biological interest, since the $O(N^6)$ scaling is still too steep. Also, some $O(N^5)$ terms of SAPT(DFT) were time-consuming. In ref 8, a partial solution to this problem was proposed based on the density-fitting (also called the resolution of identity) technique,[14−19] which allowed for reducing the scaling of the CKS dispersion energy calculations from $O(N^6)$ to $O(N^3)$. However, the construction of the TD-DFT propagators present in the expression for this energy still required $O(N^6)$ operations. If monomer-centered basis sets were employed, the propagators could be obtained just once for each monomer and then reused (after appropriate translations and rotations) for all dimer geometries. Thus, the construction of the propagators would only be a one-time expense, insignificant compared to the computational effort of obtaining the whole potential energy surface. However, for sufficiently large systems, or when only a single point on the surface is needed, calculations of the propagators could still be the bottleneck. Moreover, the convergence of the dispersion energy is much faster if the propagators are expanded in dimer-centered basis sets rather than in the monomer-centered ones.

Recently, Hesselmann et al.[20] presented an implementation of a method similar to SAPT(DFT), referred to by them as DFT-SAPT. The density-fitting techniques allowed these authors to reduce the scaling of the cost of calculating the CKS propagators to $O(N^4)$ [with $O(N^5)$ overall scaling of the full interaction energy calculation]. However, this approach cannot be applied to hybrid functionals, and the authors of ref 20 suggested using an approximate expression for the Hartree−Fock exchange term,[21] which significantly increased the computational cost. Moreover, the formulation of ref 20 is valid only if all calculations are done in the full basis set of the dimer, which may not be optimal for larger systems.

Recently, we have proposed a new algorithm for calculating the CKS propagators and dispersion energies based on density fitting that can be used with all functionals, including the hybrid ones.[22] The method scales as $O(N^5)$ for hybrid functionals and is equivalent to the formalism of ref 20 for the nonhybrid ones.

In this paper we present a complete implementation of SAPT(DFT) based on density fitting, more general than the implementation of ref 20. Also, in contrast to the latter formulation, all interaction energy components that do not depend on the CKS propagators are evaluated from molecular orbitals, using the standard expressions available in the SAPT2002 code.[23] Apart from the CKS propagators, the density fitting is also used to speed up the transformation that generates molecular integrals needed in these expressions. The outcome is a method with the overall scaling of $O(N^5)$, applicable to both nonhybrid and hybrid functionals, and capable of utilizing both dimer- and monomer-centered basis sets, including the so-called "monomer-centered-plus" bases of ref 24. The precise definition of the SAPT(DFT) approach is presented in section II. Section III discusses the density-fitting approximation used to simplify the transformation of two-electron integrals and CKS calculations. The details of the implementation and an analysis of computational costs are presented in section IV, followed by a discussion in section V of the results obtained for some model systems. Section VI contains conclusions.

II. SAPT(DFT) Method

The SAPT(DFT) method has its roots in the wave function-based SAPT, described in detail in a number of reviews.[1−3] In SAPT, the total Hamiltonian of the dimer *AB* is partitioned as

$$H = F_A + F_B + V + W_A + W_B \tag{1}$$

where F_X and W_X are the Fock operator and the intramonomer correlation operator, respectively, of monomer X ($W_X = H_X - F_X$ with H_X denoting the full Hamiltonian of monomer X), and V is the intermolecular interaction operator. A perturbation theory, starting from the product of Hartree−Fock (HF) determinants of the monomers as the zero-order wave function, gives then the interaction energy in the form of an expansion

$$E_{int} = \sum_{i=1,j=0} (E_{pol}^{(ij)} + E_{exch}^{(ij)}) \tag{2}$$

where the indices i and j denote orders with respect to the operators V and $W = W_A + W_B$, respectively. The polarization terms (with subscript "pol") result from the standard Rayleigh−Schrödinger perturbation theory, whereas the exchange terms (with subscript "exch") arise from antisymmetrization of the dimer wave function in each order. The polarization corrections of the first order in V describe the electrostatic interactions between unperturbed monomers and are therefore denoted by $E_{elst}^{(1j)}$. The second-order corrections can be split into the induction and dispersion components, $E_{pol}^{(2j)} = E_{ind}^{(2j)} + E_{disp}^{(2j)}$ and $E_{exch}^{(2j)} = E_{exch-ind}^{(2j)} + E_{exch-disp}^{(2j)}$. In most applications, it is sufficient to truncate the expansion 2 at the second order in V. If, in addition, all intramonomer correlation corrections are neglected, one obtains the following approximation to the interaction energy (termed SAPT0 without response)

$$E_{int} = E_{elst}^{(10)} + E_{exch}^{(10)} + E_{ind}^{(20)} + E_{disp}^{(20)} + E_{exch-ind}^{(20)} + E_{exch-disp}^{(20)} \tag{3}$$

All terms on the right hand side of eq 3 can be expressed in terms of integrals over HF molecular orbitals of the monomers and orbital energies. In ref 4, Williams and Chabalowski proposed to replace the HF orbitals and energies in these expressions by the ones obtained from DFT Kohn−Sham calculations, hoping that this would compensate for the neglect of intramonomer correlation in the approximation of eq 3. Formally, such an approach corresponds to splitting the dimer Hamiltonian as

$$H = K_A + K_B + V + W_A^{KS} + W_B^{KS} \tag{4}$$

(with K_X denoting the Kohn−Sham operator of monomer X

and $W_X^{KS} = H_X - K_X$) and truncating the resulting perturbation theory at zeroth order in W_X^{KS}.

The original proposal of ref 4 suffered from two fundamental problems. First, most of the commonly used exchange-correlation potentials v_{xc} do not exhibit the proper asymptotic behavior $v_{xc}(\mathbf{r}) \rightarrow -1/r + I + \epsilon_{HOMO}$, where I is the ionization potential and ϵ_{HOMO} is the highest occupied molecular orbital eigenvalue. As it was pointed out in refs 4−7, meaningful interaction energies can only be obtained after an asymptotic correction is applied to the exchange-correlation potential.

The second problem with the formulation of ref 4 was that the expression for $E_{disp}^{(20)}$ evaluated with KS orbitals and orbital energies does not correctly reproduce the dispersion energy. To remedy this flaw, it has been proposed[8,9] to make use of the generalized Casimir-Polder expression,[25−27] relating the dispersion energy to frequency-dependent density susceptibilities, $\alpha_X(\mathbf{r}, \mathbf{r}'|u)$, $X = A, B$

$$E_{disp}^{(2)} = -\frac{1}{2\pi}\int_0^\infty du \int \alpha_A(\mathbf{r}_1,\mathbf{r}'_1|\, iu)\alpha_B(\mathbf{r}_2,\mathbf{r}'_2|\, iu)\frac{d\mathbf{r}_1 d\mathbf{r}_2}{|\mathbf{r}_1 - \mathbf{r}_2|}\frac{d\mathbf{r}'_1 d\mathbf{r}'_2}{|\mathbf{r}'_1 - \mathbf{r}'_2|} \quad (5)$$

where the FDDSs are computed at imaginary frequencies iu. The expression 5 gives the exact second-order dispersion energy as long as the FDDSs are exact. Within the DFT framework, accurate FDDSs can be computed in the CKS approach. Using these FDDSs in eq 5, one obtains a quantity we shall refer to as $E_{disp}^{(2)}$(CKS), which was shown[8−10] to provide a very good approximation to the dispersion energy. Likewise, the induction energy can be computed using the expression[28]

$$E_{ind}^{(2)} = \frac{1}{2}\int \omega_B(\mathbf{r})\alpha_A(\mathbf{r},\mathbf{r}'|0)\omega_B(\mathbf{r}')d\mathbf{r}d\mathbf{r}' + \frac{1}{2}\int \omega_A(\mathbf{r})\alpha_B(\mathbf{r},\mathbf{r}'|\,0)\omega_A(\mathbf{r}')d\mathbf{r}d\mathbf{r}' \quad (6)$$

where ω_X denotes the electrostatic potential generated by monomer X:

$$\omega_X(\mathbf{r}) = \int \frac{\rho_X(\mathbf{r}')}{|\mathbf{r} - \mathbf{r}'|}d\mathbf{r}' + V_{nuc,X}(\mathbf{r}) \quad (7)$$

In the equation above, $\rho_X(\mathbf{r})$ is the electron density of monomer X, and $V_{nuc,X}(\mathbf{r})$ is the nuclear potential of X. This expression gives the exact second-order induction energy as long as $\rho_X(\mathbf{r})$ and FDDSs at zero frequency are exact. Thus, eqs 5 and 6 together give the exact second-order polarization energy. If expression 6 is computed with uncoupled KS FDDSs and the KS electron densities, the result is equivalent to the calculation of $E_{ind}^{(20)}$ with KS orbitals and orbital energies. If instead the FDDSs at the CKS level are used, one obtains a quantity which we shall refer to as $E_{ind}^{(2)}$(CKS). The KS electron densities are always obtained from asymptotically corrected calculations.

The total SAPT(DFT) interaction energy (up to second order in V) can now be defined as[10]

$$E_{int}^{SAPT(DFT)} = E_{elst}^{(1)}(KS) + E_{exch}^{(1)}(KS) + E_{ind}^{(2)}(CKS) + \tilde{E}_{exch-ind}^{(2)}(CKS) + E_{disp}^{(2)}(CKS) + \tilde{E}_{exch-disp}^{(2)}(CKS) \quad (8)$$

where the terms with CKS label result from the coupled Kohn−Sham approach, whereas the terms labeled KS are obtained by using Kohn−Sham orbitals and orbital energies to compute the corresponding quantities on the right hand side of eq 3. Since the exact expressions for the exchange-induction and exchange-dispersion corrections at the CKS level are not known, we use approximations to these quantities obtained by scaling their KS counterparts:

$$\tilde{E}_{exch-ind}^{(2)}(CKS) = E_{exch-ind}^{(2)}(KS) \times \frac{E_{ind}^{(2)}(CKS)}{E_{ind}^{(2)}(KS)} \quad (9)$$

$$\tilde{E}_{exch-disp}^{(2)}(CKS) = E_{exch-disp}^{(2)}(KS) \times \frac{E_{disp}^{(2)}(CKS)}{E_{disp}^{(2)}(KS)} \quad (10)$$

The approximate nature of these expressions is indicated by the tilde sign. The accuracy of these approximations was tested on small benchmark systems and was shown to be adequate.[10,11]

The SAPT(DFT) interaction energy of eq 8 has been shown in ref 10 to provide a very good approximation to the most accurate available values computed by wave function-based methods. The success of the method can be attributed mostly to the ability of DFT to accurately reproduce molecular densities and response properties. Since the expensive intramonomer correlation terms are avoided [in particular, a SAPT(KS) calculation includes only the expressions given in eq 3], the computational cost of SAPT(DFT) is lower than that of the conventional ab initio methods which have to include these terms to achieve acceptable accuracies. In SAPT(KS), once the integrals over molecular orbitals are available, the computation of all terms in eq 3 takes virtually negligible time compared to the regular SAPT calculation at the complete currently available level of theory. This is due to the $O(N^5)$ vs $O(N^7)$ scaling of the two methods, and in addition to the fact that for $E_{exch-disp}^{(2)}$, the only correction in eq 3 that scales as $O(N^5)$, the precise scaling is $O(o^3v^2)$, with o and v denoting the numbers of occupied and virtual orbitals, and in most cases $o \ll v$. In consequence, SAPT(KS) calculations are dominated by the integral transformation which, for the corrections needed, scales as $O(on^4)$, where $n = o + v$. In SAPT(DFT), however, there are three steps which, for most systems, are more time-consuming than the transformation. (*a*) The construction of the TD-DFT matrices which requires a numerical evaluation of four index integrals involving the derivative of v_{xc} and scales as $O(o^2v^2g)$, where g is the number of integration points. Since g increases with the system size, this integration is an $O(N^5)$ process. (*b*) The evaluation of the TD-DFT propagators, which requires multiplications and inversions of large matrices and scales as $O(N^6)$. (*c*) The calculation of the CKS dispersion energy from the propagators. These three bottlenecks were addressed in refs 8, 10, 20, and 22 and sped up by using density fitting techniques and iterative matrix inversion methods, resulting in scalings of at the most

$O(N^5)$ and greatly reduced prefactors. With these improvements, the integral transformation becomes the most time-consuming step of a SAPT(DFT) calculation for a wide range of systems. In the following sections, we will show how the cost of the transformation can be reduced using density fitting ideas. We will also describe changes that had to be implemented to use the asymptotic correction with the DALTON[29] set of computer codes and develop the density fitting method for the CKS induction energy.

III. Density Fitting Approximation

Two-electron integrals occurring in electronic structure theory can be written in terms of generalized densities, defined as

$$\rho_{ij}(\mathbf{r}) = \phi_i(\mathbf{r})\phi_j(\mathbf{r}) \tag{11}$$

where ϕ_i and ϕ_j are any molecular orbitals of the system considered. The idea of density fitting is to approximate the density ρ_{ij} by

$$\tilde{\rho}_{ij}(\mathbf{r}) = \sum_K^{N_{\text{aux}}} D_K^{ij}\chi_K(\mathbf{r}) \tag{12}$$

where χ_K, $K = 1,\ldots, N_{\text{aux}}$, are auxiliary (fitting) basis functions, usually atom-centered Gaussian orbitals. We assume for simplicity that the auxiliary basis set is identical for all the densities, but, in general, it may depend on i, j. The error introduced by the fitting can be quantified in terms of the functional

$$\Delta_{ij} = \int \mathrm{d}\mathbf{r}_1\mathrm{d}\mathbf{r}_2\,[\rho_{ij}(\mathbf{r}_1) - \tilde{\rho}_{ij}(\mathbf{r}_1)][\rho_{ij}(\mathbf{r}_2) - \tilde{\rho}_{ij}(\mathbf{r}_2)]w(\mathbf{r}_1,\mathbf{r}_2) \tag{13}$$

where $w(\mathbf{r}_1,\mathbf{r}_2)$ is a weight factor. In our implementation, we set $w(\mathbf{r}_1,\mathbf{r}_2) = 1/|\mathbf{r}_1 - \mathbf{r}_2|$, as recommended in ref 16 for fitting electron repulsion integrals. The fit coefficients D_K^{ij} are obtained by minimizing the functional 13, which leads to the following expression

$$D_K^{ij} = \sum_L [\mathbf{J}^{-1}]_{KL}(ij|\,L) \tag{14}$$

where

$$(ij|L) = \int \mathrm{d}\mathbf{r}_1\mathrm{d}\mathbf{r}_2\,\frac{\phi_i(\mathbf{r}_1)\phi_j(\mathbf{r}_1)\chi_L(\mathbf{r}_2)}{|\mathbf{r}_1 - \mathbf{r}_2|} \tag{15}$$

$$J_{LK} = \int \mathrm{d}\mathbf{r}_1\mathrm{d}\mathbf{r}_2\,\frac{\chi_L(\mathbf{r}_1)\chi_K(\mathbf{r}_2)}{|\mathbf{r}_1 - \mathbf{r}_2|} \tag{16}$$

IV. Implementation

A complete SAPT(DFT) calculation for one dimer geometry consists of several steps implemented as separate programs. First, the Kohn−Sham calculations are performed for both monomers, followed by the integral transformation. The transformed integrals are then used to generate the CKS propagators and to obtain the induction and dispersion energies. Finally, the standard code from the SAPT2002 suite[23] is invoked to compute corrections labeled "KS" in eqs 8−10. In the following sections, each of these steps is discussed in more detail.

A. Asymptotically Corrected Kohn−Sham Calculation. In the current version of SAPT(DFT) codes, the Kohn−Sham orbitals and orbital energies for monomers are obtained from the DALTON program.[29] The previous version was interfaced with the CADPAC program[30] which included the asymptotic correction in Kohn−Sham calculations. We have implemented this correction in DALTON in the following way. Using the density $\rho(\mathbf{r})$ from uncorrected Kohn−Sham calculations, the Fermi-Amaldi asymptotic potential[31] is computed as

$$v_{\text{xc,FA}}(\mathbf{r}) = -\frac{1}{N_{\text{el}}}\int \frac{\rho(\mathbf{r}')}{|\mathbf{r} - \mathbf{r}'|}d\mathbf{r}' \tag{17}$$

where N_{el} denotes the number of electrons. This potential is shifted to obtain the final asymptotic form

$$v_{\text{xc,as}}(\mathbf{r}) = v_{\text{xc,FA}}(\mathbf{r}) + I + \epsilon_{\text{HOMO}} \tag{18}$$

The ionization potential I can be taken from experiment or from a separate ab initio or DFT calculation. The splicing scheme of Tozer and Handy[31] is then used to connect $v_{\text{xc,as}}(\mathbf{r})$ with the standard short-range part. For the splicing scheme, we used Bragg radii factors of 3.0 and 4.0 as recommended in ref 32. The Fermi-Amaldi asymptotic potential will not represent well the true asymptotic potential for large molecules, in particular for long polymers. It has been shown in ref 11 that the asymptotic correction improves the results for the water dimer, but its effects are small for the carbon dioxide dimer. For larger molecules to which SAPT(DFT) has been applied, there are no sufficiently accurate benchmarks to determine the accuracy of the Fermi-Amaldi approximation. It is possible, however, that the detailed shape of $v_{\text{xc,as}}(\mathbf{r})$ is not very important as long as the energy shift in eq 18 is correct. We plan further investigations of these problems in near future.

The asymptotically corrected v_{xc} is computed on a grid and then used to obtain Kohn−Sham orbitals. These steps are repeated until convergence (with unchanged $v_{\text{xc,FA}}$, but with updated ϵ_{HOMO}). The use of asymptotically corrected v_{xc} requires modifications in Kohn−Sham procedures. In the standard Kohn−Sham DFT, v_{xc} is defined as the functional derivative of the exchange-correlation energy $E_{\text{xc}} = \int F_{\text{xc}}(\rho,\nabla\rho)d\mathbf{r}$, where F_{xc} is the exchange-correlation kernel. In generalized-gradient approximation (GGA) Kohn−Sham calculations, v_{xc} is not evaluated explicitly. Instead, integration by parts is used in all integrals involving v_{xc} to avoid second derivatives of the density. This method is not applicable to asymptotically corrected v_{xc} since F_{xc} is now not known in the asymptotic region. Therefore, we had to modify DALTON codes to be able to use the explicit formula[33] (in the short-range region)

$$v_{\text{xc}} = \frac{\partial F_{\text{xc}}}{\partial\rho} - \zeta\frac{\partial^2 F_{\text{xc}}}{\partial\zeta\partial\rho} - \frac{1}{\zeta}\frac{\partial F_{\text{xc}}}{\partial\zeta}\rho_{\gamma\gamma} - \frac{1}{\zeta^2}\left(\frac{\partial^2 F_{\text{xc}}}{\partial\zeta^2} - \frac{1}{\zeta}\frac{\partial F_{\text{xc}}}{\partial\zeta}\right)\rho_\gamma\rho_{\gamma\delta}\rho_\delta \tag{19}$$

where ρ_δ and $\rho_{\delta\gamma}$ are the first and second derivatives, respectively, of the density with respect to Cartesian coor-

dinates δ, γ, $\zeta = (\rho_x^2 + \rho_y^2 + \rho_z^2)^{1/2}$ is the length of the density gradient and explicit summation of repeated indices is assumed.

The coefficients of the converged asymptotically corrected Kohn−Sham orbitals and orbital energies are stored on disk for further processing. If a monomer-centered basis set is used, one-electron atomic integrals in a dimer basis set are computed in the next step (if a dimer-centered basis set is used, these integrals are already computed during monomer DFT calculations).

B. TD-DFT Kernel Integral. For the purpose of the TD-DFT calculations, it is necessary to evaluate, for each monomer, the matrix elements of the form[34,35]

$$\int \phi_a(\mathbf{r})\phi_r(\mathbf{r})\phi_{a'}(\mathbf{r})\phi_{r'}(\mathbf{r})\frac{\partial v_{xc}}{\partial \rho}d\mathbf{r} \tag{20}$$

where a, a' and r, r' refer to the occupied and virtual KS orbitals, respectively. Notice that in the asymptotically corrected SAPT(DFT) approach, the standard, uncorrected v_{xc} is used in eq 20 since the derivative of $v_{xc,ac}$ cannot be computed in practice. However, the orbitals are from asymptotically corrected KS calculations.

The cost of calculating eq 20 scales as $O(o^2v^2g)$, i.e, an overall $O(N^5)$ scaling, and is quite significant since the numerical integration requires very fine grids. References 20 and 22 described the implementation of the density-fitting in the evaluation of the integral 20. If the product $\phi_{a'}\phi_{r'}$ is approximated using eq 12, one only needs to compute and store the matrix elements

$$\int \phi_a(\mathbf{r})\phi_r(\mathbf{r})\chi_K(\mathbf{r})\frac{\partial v_{xc}}{\partial \rho}d\mathbf{r} \tag{21}$$

which reduces the scaling by a factor of ov/N_{aux}. The integration in eq 21 is performed using the same quadrature as in the DFT calculations.

We have implemented in ref 22 the density fitting only for the local-density approximation (LDA) kernels in eq 20 [all other stages in a TD-DFT/GGA calculation contain the proper GGA v_{xc}]. The use of the LDA kernel has been shown to result in small differences, below 1%, in dispersion energies compared to the GGA kernels.[10] This accuracy should be more than sufficient for the intended applications of the density-fitting technique, i.e., for very large systems. An implementation of this technique to GGA kernels is possible but would be significantly more complicated than in the LDA case. One should first point out that the form of integral 20 is strictly speaking valid only for the LDA v_{xc} potential, and the derivative is then just the standard partial derivative. For GGA kernels, this integral cannot be written as a product of four orbitals times a function of $\boldsymbol{r}$ independent of the indices of the orbitals. The most straightforward form of this integral [eq 25 in ref 36] includes terms containing a product of two orbitals, up to second derivatives of two other orbitals, up to second derivatives of density, and up to third derivatives of F_{xc}. This expression would be significantly more time-consuming to compute compared to the LDA kernel. If integration by parts is applied, one can obtain a more manageable integral containing only the first derivatives of density and orbital products and second derivatives of F_{xc}, see eq 23 in ref 33. Unfortunately, an application of density fitting techniques to this integral would be difficult since some terms do not contain orbital products but only their derivatives, and fitting such derivatives is numerically more difficult than fitting orbital products only.

C. Integral Transformation. All quantities in eq 8 are given in terms of one- and two-electron integrals over molecular orbitals (and propagators for the CKS terms). After the techniques presented in refs 10, 20, and 22 (see also section IV D) are applied and the $O(N^6)$ terms eliminated, the two-electron transformation with the nominal scaling of $O(N^5)$ becomes the most time-consuming part of SAPT(DFT) for a wide range of systems. Although there are other components scaling as $O(N^5)$ remaining, the conventional transformation has the largest prefactor. However, as it will be shown below, the transformation can greatly benefit from density fitting.

The objective of the two-electron transformation is to compute molecular integrals

$$(ij|kl) = \int d\mathbf{r}_1 d\mathbf{r}_2 \frac{\phi_i(\mathbf{r}_1)\phi_j(\mathbf{r}_1)\phi_k(\mathbf{r}_2)\phi_l(\mathbf{r}_2)}{|\mathbf{r}_1 - \mathbf{r}_2|} \tag{22}$$

where i, j, k, and l label molecular (occupied or virtual) orbitals of monomer A or B, expanded in terms of atomic (and possibly midbond) basis functions ψ_μ, e.g., $\phi_p = \sum_\mu c_{\mu p}\psi_\mu$. The integral written above can be expressed using the densities of eq 11 as

$$(ij|kl) = \int d\mathbf{r}_1 d\mathbf{r}_2 \frac{\rho_{ij}(\mathbf{r}_1)\rho_{kl}(\mathbf{r}_2)}{|\mathbf{r}_1 - \mathbf{r}_2|} \tag{23}$$

By inserting eq 12 into eq 23, one obtains

$$(ij|kl) \approx \sum_{KL} D_K^{ij} D_L^{kl} J_{KL} = \sum_K D_K^{ij} \tilde{D}_K^{kl} \tag{24}$$

where

$$\tilde{D}^{ij}{}_K = \sum_L D_{KL}^{ij} J_L \tag{25}$$

with J_{KL} defined in eq 16. Since we use dimer-centered auxiliary basis sets, χ_K and χ_L are always from the same basis set. By inserting eq 14 into eq 25, we obtain

$$\tilde{D}_K^{kl} = (kl|K) \tag{26}$$

and eq 24 then reads

$$(ij|kl) \approx \sum_K D_K^{ij}(kl|K) \tag{27}$$

The integrals $(ij|K)$ are obtained by transforming the 3-center atomic orbital (AO) integrals $(\mu\nu|K)$

$$(\mu j|K) = \sum_\nu c_{\nu j}(\mu\nu|K) \tag{28}$$

$$(ij|K) = \sum_\mu c_{\mu i}(\mu j|K) \tag{29}$$

where c_{vi} are molecular (Kohn−Sham) orbital coefficients and $(\mu i|K)$ are partially transformed integrals.

In our implementation, the 3-center $(\mu\nu|K)$ and 2-center J_{KL} integrals are first calculated in the full, dimer-centered basis set using the integral package adopted from the GAMESS-US code.[37] If monomer-centered basis sets are used, the required integrals for monomer A and B are also extracted from this file. Then, the 3-center integrals are contracted according to eq 28, where the orbital coefficients may correspond to the monomer A or B depending on the computed integral. This step scales as $O(wn^2N_{\mathrm{aux}})$, where $w = o$ or v depending on the contraction index i, and n is the total number of orbitals $n = o + v$. One cannot avoid i being a virtual index for $(ab|rs)$-type integrals only, where a, b denote occupied and r, s denote virtual indices (these integrals are required for the TD-DFT matrices with hybrid functionals and for the third-order terms, see section IV D). Since in this case the resulting set of semitransformed integrals $(\mu j|K)$ can be large, the transformation is done out-of-core, i.e., with only a part of the integral matrix stored in memory. Although such a transformation requires more disk operations than an in-core one, it scales only as $O(N^4)$, and, therefore, for larger systems it is only a small part of the whole calculation. The intermediate semitransformed integrals are stored and reused for all integrals that share the same intermediate. Next, the contractions of eq 29 are performed, and the resulting 3-center integrals are also stored. This step scales as $O(ww'N_{\mathrm{aux}})$, where $w' = o$ or v depending on the contraction index j. The smaller sets of the 3-index intermediates are stored in memory, whereas the larger ones are stored on disk and then read in batches that can fit into memory.

After the integrals are computed, the matrix $\mathbf{J}$ of eq 16 is inverted in an $O(N_{\mathrm{aux}}^3)$ step, and then the fit coefficients of eq 14 are computed at a cost of $O(ww'N_{\mathrm{aux}}^2)$ (with w, w' equal to o or v) and stored on disk as the file size is $ww'N_{\mathrm{aux}}$ which can be fairly large. Finally, the transformed 4-index integrals are obtained from eq 27 and stored on disk. This final step scales at most as $O(o^2v^2N_{\mathrm{aux}})$, or $O(N^5)$, the highest formal scaling in the whole transformation procedure. The o^2v^2 part of the scaling is due to the fact that molecular integrals required by SAPT(DFT) have no more than two virtual indices.

Although the transformation described above has the same nominal $O(N^5)$ scaling as the conventional transformation, the operation count is reduced compared to the latter one [the cost of the latter procedure is $O(on^4)$]. Moreover, the density fitting brings additional advantages[19] due to the smaller size of the atomic integral file (3-index, instead of 4-index), reducing the IO-operation count and simplifying the usage of very efficient matrix algebra routines in eq 24.

D. CKS Induction Energies. We have shown in ref 22 how the CKS dispersion energies can be efficiently computed using density-fitting techniques. Here we apply the same method to the CKS induction energies. The CKS FDDS appearing in eqs 5 and 6 can be expressed[35,38] as linear combinations of products of occupied and virtual orbitals of a given monomer. For monomer A we have

$$\alpha_A(\boldsymbol{r},\boldsymbol{r}'|iu) = \sum_{ara'r'} C^A_{ar,a'r'}(iu)\phi_a(\boldsymbol{r})\phi_r(\boldsymbol{r})\phi_{a'}(\boldsymbol{r}')\phi_{r'}(\boldsymbol{r}') \quad (30)$$

where the coefficient matrix $\mathbf{C}^{\mathrm{A}}(iu)$ is obtained from the equation

$$(\mathbf{H}^{(2)}\mathbf{H}^{(1)} + u^2\mathbf{I}_{ov})\mathbf{C}^A(iu) = -4\mathbf{H}^{(2)} \quad (31)$$

with $\mathbf{I}_{ov}$ denoting the $ov \times ov$ unit matrix and the matrices $\mathbf{H}^{(i)}$, $i = 1, 2$, given by[34]

$$\mathbf{H}^{(1)} = \mathbf{d} + 4\mathbf{H}_0^{(1)} + \mathbf{H}_{\mathrm{r}}^{(1)} \quad (32)$$

$$\mathbf{H}^{(2)} = \mathbf{d} + \mathbf{H}_{\mathrm{r}}^{(2)} \quad (33)$$

The diagonal matrix $\mathbf{d}$ is defined in terms of orbital energies ϵ_p as $\mathbf{d}_{ar,a'r'} = \delta_{aa'}\delta_{rr'}(\epsilon_r - \epsilon_a)$, whereas the remaining matrices are given by[34]

$$(\mathbf{H}_0^{(1)})_{ar,a'r'} = (ar|a'r') + \int \phi_a\phi_r\phi_{a'}\phi_{r'}\frac{\partial v_{\mathrm{xc}}}{\partial\rho}d\mathbf{r} \quad (34)$$

$$(\mathbf{H}_{\mathrm{r}}^{(1)})_{ar,a'r'} = -\xi[(aa'|rr') + (ar'|a'r)] \quad (35)$$

$$(\mathbf{H}_{\mathrm{r}}^{(2)})_{ar,a'r'} = -\xi[(aa'|rr') - (ar'|a'r)] \quad (36)$$

where $0 \le \xi \le 1$ is the fraction of the Hartree−Fock exchange applied in a given DFT functional. Notice that although we use LDA kernel in eq 34 in the density-fitted approach, the parameter ξ is the same as in the hybrid DFT method applied. The exchange part of the LDA's v_{xc} is appropriately scaled. Some terms representing current density, which give negligible contributions for the problems considered here,[35] have been neglected in $\mathbf{H}^{(2)}$. Equations analogous to eqs 30−36—with orbitals and orbital energies of monomer A replaced by those of monomer B—describe the propagator $\alpha_B(\boldsymbol{r},\boldsymbol{r}'|iu)$.

To place calculations of the CKS induction energies in the context of the complete SAPT(DFT) calculations, let us briefly recall the approach of refs 8, 10, and 22 for the CKS dispersion energies. Inserting expansions 30 for monomers A and B into formula 5, the following expression for the CKS dispersion energy is obtained

$$E_{\mathrm{disp}}^{(2)}(\mathrm{CKS}) = -\frac{1}{2\pi}\int_0^\infty du \sum_{ara'r'bsb's'} C^A_{ar,a'r'}(iu)\, C^B_{bsb's'}(iu)(ar|bs),(a'r'|b's') \quad (37)$$

The time requirements of expression 37 and the solution of eq 31 both scale as $O(o^3v^3)$ or $O(N^6)$. Thus, for large o and v, evaluation of $E_{\mathrm{disp}}^{(2)}$(CKS) from eq 37 becomes the most time-consuming step of the SAPT(DFT) calculation. It should be emphasized at this point that the calculation of dispersion energy according to formula 37 requires the *full* propagator matrices $\mathbf{C}^A(iu)$ and $\mathbf{C}^B(iu)$ computed at a number of imaginary frequencies. This is in contrast to typical TD-DFT calculations, where only a *vector* quantity $\mathbf{C}^{\mathrm{X}}\mathbf{w}$ is of interest, where $\mathbf{w}$ is a column vector of ov matrix elements representing some perturbation of the system. Multiplying both sides of eq 31 on the right by $\mathbf{w}$, one obtains a system of linear

equations for $\mathbf{C}^X\mathbf{w}$ with the vector $-4\mathbf{H}^{(2)}\mathbf{w}$ as the right-hand side. Such a system can then be solved using iterative techniques[39,40] involving only matrix-vector multiplications and scaling as $(ov)^2$ or $O(N^4)$. A procedure of this type will be employed by us to compute the CKS induction energy. The scaling of expression 37 can be reduced to $O(N^3)$ if the two-electron integrals are approximated with density fitting.[8,10] One then obtains

$$E_{\mathrm{disp}}^{(2)} = -\frac{1}{2\pi}\int_0^\infty du \sum_{KL}^{N_{\mathrm{aux}}^A}\sum_{K'L'}^{N_{\mathrm{aux}}^B} \tilde{C}_{KL}^A(iu)\,\tilde{C}_{K'L'}^B(iu) J_{KK'}J_{LL'} \quad (38)$$

where the $N_{\mathrm{aux}}^X \times N_{\mathrm{aux}}^X$ matrix $\tilde{\mathbf{C}}^X$, $X = A, B$, is the result of the transformation

$$\tilde{\mathbf{C}}^X \equiv (\mathbf{D})^t\mathbf{C}^X\mathbf{D} \quad (39)$$

with $\mathbf{D}$ being the $ov \times N_{\mathrm{aux}}^X$ density-fitting coefficient matrix of monomer X, given by eq 14 (for simplicity of discussion we will further assume that $N_{\mathrm{aux}}^A = N_{\mathrm{aux}}^B = N_{\mathrm{aux}}$). Although the cost of performing transformation 39 is $O(o^2v^2N_{\mathrm{aux}})$ and that of evaluating expression 38 is only $O(N_{\mathrm{aux}}^3)$, the overall scaling of dispersion energy is still $O(N^6)$, due to $O(o^3v^3)$ cost of matrix operations necessary to solve eq 31 for $\mathbf{C}^X$. In ref 22 it has been shown that the latter step can be bypassed, and $\tilde{\mathbf{C}}^X$ can be obtained directly from a fast-converging iterative procedure scaling as $O(o^2v^2N_{\mathrm{aux}})$, or $O(N^5)$, in the case of hybrid functionals ($\xi \neq 0$). For nonhybrid functionals ($\xi = 0$), the iterative algorithm reduces to a one-step procedure, identical to the one described in ref 20, scaling as $O(ovN_{\mathrm{aux}}^2)$, or $O(N^4)$. Thus, using density fitting and the techniques of ref 22, the $E_{\mathrm{disp}}^{(2)}$(CKS) energy is obtained at a cost of at most $O(N^5)$. It has been shown[10,20,22] that the errors in this quantity resulting from density fitting approximation and truncation of the iterative scheme are negligible even if $N_{\mathrm{aux}} \ll ov$.

Returning now to the CKS induction energy, $E_{\mathrm{ind}}^{(2)}$(CKS), the first term on the right hand side of eq 6 can be rewritten using the orbital representation 30 of the CKS propagator $\alpha_A(\mathbf{r}_1, \mathbf{r}_1'|0)$

$$E_{\mathrm{ind}}^{(2)}(A \leftarrow B) = \frac{1}{2}\int \omega_B(\mathbf{r})\alpha_A(\mathbf{r},\mathbf{r}'|0)\omega_B(\mathbf{r}')d\mathbf{r}d\mathbf{r}' = \frac{1}{2}\boldsymbol{\omega}^t\mathbf{C}^A(0)\boldsymbol{\omega} = \frac{1}{2}\boldsymbol{\omega}^t\mathbf{Z} \quad (40)$$

where we used the definition $\mathbf{Z} \equiv \mathbf{C}^A(0)\boldsymbol{\omega}$ and $\mathbf{C}^A(0)$ is obtained by solving eq 31 at zero frequency. The ov elements of the vector $\boldsymbol{\omega}$ are given by

$$\omega_{ar} = \int \phi_a(\mathbf{r})\phi_r(\mathbf{r})\omega_B(\mathbf{r})d\mathbf{r} \quad (41)$$

(Analogous expressions for $E_{\mathrm{ind}}^{(2)}(B \leftarrow A)$ can be obtained by properly exchanging monomer indices). Setting $u = 0$ in eq 31, then multiplying both sides of this equation on the right by ω and on the left by $(\mathbf{H}^{(2)})^{-1}$, one finds that $\mathbf{Z}$ satisfies the equation

$$\mathbf{H}^{(1)}\mathbf{Z} = -4\boldsymbol{\omega} \quad (42)$$

The matrix $\mathbf{H}_0^{(1)}$, eq 34, involving the four-index integrals considered in section IV B, can be written using eqs 12 and 21 as $\mathbf{FD}^t$, where the elements of the $ov \times N_{\mathrm{aux}}$ matrix $\mathbf{F}$ are defined as

$$F_{ar,K} = (ar|K) + \int \phi_a(\mathbf{r})\phi_r(\mathbf{r})\chi_K(\mathbf{r})\frac{\partial v_{\mathrm{xc}}}{\partial \rho}d\mathbf{r} \quad (43)$$

Equation 42 then becomes

$$(\mathbf{d} + 4\mathbf{FD}^t + \mathbf{H}_{\mathrm{r}}^{(1)})\mathbf{Z} = -4\boldsymbol{\omega} \quad (44)$$

Although eq 44 is simpler than its equivalent in the case of dispersion energy calculations [cf. eq 14 of ref 22], its direct solution scales also as $(ov)^3$. However, the matrix $\boldsymbol{\Lambda} \equiv \mathbf{d} + 4\mathbf{FD}^t$ can be inverted at a much lower cost. This can be achieved by using eq 16 in ref 22 to write the inverse of $\boldsymbol{\Lambda}$ as

$$\boldsymbol{\Lambda}^{-1} = \mathbf{d}^{-1} - 4\mathbf{d}^{-1}\mathbf{F}(\tilde{\mathbf{I}} + 4\mathbf{D}^t\mathbf{d}^{-1}\mathbf{F})^{-1}\mathbf{D}^t\mathbf{d}^{-1} \quad (45)$$

where $\tilde{\mathbf{I}}$ is the $N_{\mathrm{aux}} \times N_{\mathrm{aux}}$ unit matrix. The operations involved in eq 45 are performed in the following way. First, the matrix in parentheses is constructed from matrices $\mathbf{F}$ and $\mathbf{D}$ stored in memory, which requires matrix−matrix multiplications scaling as N_{aux}^2ov, or, equivalently, $O(N^4)$. The inverse of this matrix is then obtained at a cost proportional to N_{aux}^3 and stored in memory. The remaining matrix multiplications in eq 45 could be performed at the cost $O(N^4)$. However, matrix $\boldsymbol{\Lambda}^{-1}$ is never computed explicitly. Instead, its action on a vector of length ov is evaluated as a sequence of matrix-vector multiplications using consecutive matrices in eq 45, with scaling not exceeding $N_{\mathrm{aux}}ov$, or $O(N^3)$.

Application of $\boldsymbol{\Lambda}^{-1}$ to both sides of eq 44 written as $\boldsymbol{\Lambda}\mathbf{Z} = -4\boldsymbol{\omega} - \mathbf{H}_{\mathrm{r}}^{(1)}\mathbf{Z}$ leads to an iterative process

$$\mathbf{Z}_{n+1} = \mathbf{Z}_0 - \boldsymbol{\Lambda}^{-1}\mathbf{H}_{\mathrm{r}}^{(1)}\mathbf{Z}_n \quad (46)$$

with $\mathbf{Z}_0 = -4\boldsymbol{\Lambda}^{-1}\omega$. The iterations stop when the length of dimensionless vector $\mathbf{Z}$ changes by less than a predefined threshold, set equal to 10^{-12}. For nonhybrid functionals, i.e., when $\mathbf{H}_{\mathrm{r}}^{(1)} = 0$, the solution $\mathbf{Z} = \mathbf{Z}_0$ is obtained in a one-step procedure. The term $\boldsymbol{\Lambda}^{-1}\mathbf{H}_{\mathrm{r}}^{(1)}\mathbf{Z}_n$ is computed in each iteration by first evaluating the vector $\mathbf{H}_{\mathrm{r}}^{(1)}\mathbf{Z}_n$ and then multiplying this vector by $\boldsymbol{\Lambda}^{-1}$ in the way described above. The former of these steps, scaling as $(ov)^2$ or $O(N^4)$, is the most demanding part of the whole calculation of the induction energy. Still, this scaling is much more favorable than the $O(N^5)$ requirements of several other steps in a SAPT(DFT) calculation. It should be also mentioned that there is no need to store the entire matrix $\mathbf{H}_{\mathrm{r}}^{(1)}$ in memory in order to perform a matrix-vector multiplication. Instead, a number of rows of this matrix is read in at a time, depending on available memory, and the corresponding components of the resultant vector $\mathbf{H}_{\mathrm{r}}^{(1)}\mathbf{Z}_n$ are evaluated. This is important for larger systems, where the $(ov)^2$ storage requirement would be sizable.

E. SAPT(KS) Terms. All terms $E_{\mathrm{a}}^{(n)}$(KS) in eqs 8 and 10, where 'a' stands for any of the electrostatic, induction, dispersion, or exchange terms, are computed from the standard SAPT expressions for $E_{\mathrm{a}}^{(n0)}$ in which the Hartree−

Fock orbitals and orbital energies have been replaced by their Kohn−Sham counterparts. The relevant expressions, presented in ref 41, are evaluated using the existing routines from the SAPT2002 program.[23] The required one- and two-electron integrals over KS molecular orbitals are obtained from integrals over atomic orbitals as described in section IV C. The calculation of the KS terms from molecular orbitals is quite fast, even though, as discussed earlier, the most time-consuming of these terms, $E^{(2)}_{\mathrm{exch-disp}}$(KS), scales as $O(o^3v^2)$, or $O(N^5)$. However, since normally $o \ll v$, evaluation of this term is much faster than that of the other $O(N^5)$ parts of a SAPT(DFT) calculation.

F. Higher Orders in *V*. In some cases, the effects of higher orders in V are significant and have to be included. In past applications of SAPT, these effects have been usually estimated as the difference between the Hartree−Fock interaction energy and the sum of SAPT terms up to the second order in V that do not include any correlation effects

$$\delta E^{\mathrm{HF}}_{\mathrm{int}} = E^{\mathrm{HF}}_{\mathrm{int}} - (E^{(10)}_{\mathrm{elst}} + E^{(10)}_{\mathrm{exch}} + E^{(20)}_{\mathrm{ind,resp}} + E^{(20)}_{\mathrm{exch-ind,resp}}) \quad (47)$$

where the quantities with the subscript "resp" are computed including the coupled Hartree−Fock-type response of monomer orbitals to the field of the partner. The quantity $\delta E^{\mathrm{HF}}_{\mathrm{int}}$ is a good approximation to higher-order terms in case of molecules with a significant induction contribution. For molecules with a small induction contribution, the benefits of including $\delta E^{\mathrm{HF}}_{\mathrm{int}}$ are not clear, and, in some cases, like rare gas dimers, this component does not approximate the third and higher-order effects well. Although including $\delta E^{\mathrm{HF}}_{\mathrm{int}}$ does not increase the scaling beyond that of SAPT(DFT), in most cases the supermolecular SCF, together with the terms of regular SAPT listed in eq 47, form a significant part of the whole calculation.

Recently, explicit formulas for the third-order terms have been derived and implemented.[42] The sum of the induction and exchange-induction terms, $E^{(30)}_{\mathrm{ind}} + E^{(30)}_{\mathrm{exch-ind}}$, can provide a major part of high-order effects. Preliminary tests with wave function-based SAPT[42] showed that this approach leads to more accurate interaction energies for nonpolar systems than the use of $\delta E^{\mathrm{HF}}_{\mathrm{int}}$. The two corrections can be straightforwardly computed in the SAPT(KS) approach. The density-fitting formalism has been applied to obtain the molecular integrals needed [with $O(o^2v^2N_{\mathrm{aux}})$ scaling]. The use of $E^{(30)}_{\mathrm{ind}}$ and $E^{(30)}_{\mathrm{exch-ind}}$ does not increase the overall scaling of SAPT(DFT) as the cost of these corrections scales as $O(o^2v^2)$ and $O(o^3v^2)$, respectively. Since the third-order terms in the KS version have not yet been sufficiently tested, we have not included them in the numerical results presented below.

G. Advantages of Density Fitting. Concluding this section, let us shortly summarize the advantages of using density-fitting with SAPT(DFT). Compared to the approach without density fitting, the method gains an order of magnitude better scaling. The cost of the dispersion energy calculation reduces from $O(o^3v^3)$ to $O(o^2v^2N_{\mathrm{aux}})$, and the computation of the matrix elements involving the exchange-correlation kernel requires $O(ovN_{\mathrm{aux}}g)$ operations instead of $O(o^2v^2g)$ needed in the standard case. Scaling of the most expensive step of the transformation is reduced from on^4 to $o^2v^2N_{\mathrm{aux}}$. Memory requirements of transformation and of the CKS-based calculations are also significantly reduced since most operations are performed on 3-index objects which fit in memory easier than the 4-index ones used in the standard SAPT(DFT). With reduced memory usage, it is straightforward to apply highly optimized matrix−matrix multiplication BLAS routines,[43] which results in further speedups. Since no 4-index AO integrals are needed, only 3-index and relatively small (o^2v^2) 4-index objects have to be stored on disk. This results in a very significant reduction of disk usage and the input/output (I/O) operation count.

V. Results and Discussion

A. Numerical Details. We have tested the density-fitting SAPT(DFT) approach mainly on the example of the benzene dimer for which we have considered three intermolecular separations. Additional tests have been performed for near-equilibria configurations of the argon dimer, the water dimer, and the dimer of cyclotrimethylene trinitramine, $(CH_2-N-NO_2)_3$, known also under the name RDX. The Kohn−Sham orbitals were obtained using the PBE0 functional[44,45] with the Fermi-Amaldi asymptotic correction and Tozer-Handy splicing scheme[31,46] computed with the experimental ionization potentials[47] equal to 0.3397, 0.5791, and 0.4638 hartree for C_6H_6, Ar, and H_2O, respectively, and 0.373 hartree for RDX computed using PBE0 as the energy difference between the neutral molecule and the cation. In all calculations the LDA kernel was used in eqs 20 and 21. The DFT calculations were performed using the DALTON code[29] with the aug-cc-pV*X* Z, $X = 2$, 3 and cc-pVDZ bases of Dunning et al.[48] In some cases, these basis sets were centered on both monomers and extended with a set of midbond functions, placed halfway between the centers of mass of the monomers. A dimer-centered basis set (DCBS) containing midbond functions will be referred to as DC$^+$BS. In another approach, referred to as MC$^+$BS[24], orbitals of a given monomer were expanded in terms of this monomer's own basis, the midbond functions, and the isotropic part (i.e., with the polarization functions removed) of the basis of the other monomer. Our set of midbond functions (3*s*3*p*2*d*2*f*) consisted of three *s* and three *p* shells with exponents (0.9, 0.3, 0.1) and of two *d* and two *f* shells with exponents (0.6, 0.2). The density fitting approximation was accomplished for all SAPT terms using auxiliary basis sets of ref 49, fitted to the second-order Møller−Plesset (MP2) results for atoms and corresponding to the principal orbital bases applied. As it was the case with the underlying principal bases, the auxiliary ones were usually extended with a set of midbond functions, containing five each of uncontracted *spd* shells with exponents (1.8, 1.2, 0.6, 0.4, 0.2), four *f* shells with exponents (1.5, 0.9, 0.5, 0.3), and three *g* shells with exponents (1.5, 0.9, 0.3), chosen to approximately reproduce the products of midbond functions. Only the DCBS and DC$^+$BS types (but not MC$^+$BS) were used for auxiliary bases (even if the principal basis set was of MC$^+$BS type). Although the MC$^+$BS auxiliary functions would reduce slightly the computational cost of some parts of the code, the resulting inability of reusing certain intermediates during the transformation and a small loss of accuracy would outweigh the

Table 1: Decomposition of the SAPT(DFT) Interaction Energy Obtained with Density Fitting for the Benzene Dimer in a "Sandwich" Configuration with Monomers in the Geometry of Ref 50[a]

	$R = 3.2$ Å		$R = 3.85$ Å		$R = 5.0$ Å	
$E_{elst}^{(1)}$(KS)	−6.1931	(−0.0011)	0.1362	(0.0019)	0.5550	(−0.0009)
$E_{exch}^{(1)}$(KS)	21.8896	(0.0021)	3.2976	(0.0006)	0.0944	(0.0001)
$E_{ind}^{(2)}$(CKS)	−8.7913	(0.0002)	−1.1067	(0.0000)	−0.0626	(−0.0000)
$\tilde{E}_{exch-ind}^{(2)}$(CKS)	8.4937	(−0.0002)	0.8947	(−0.0000)	0.0121	(0.0000)
$E_{disp}^{(2)}$(CKS)	−15.0480	(0.0037)	−5.3452	(0.0008)	−1.1005	(−0.0000)
$\tilde{E}_{exch-disp}^{(2)}$(CKS)	2.3979	(−0.0009)	0.4480	(−0.0002)	0.0179	(−0.0000)
$E_{int}^{SAPT(DFT)}$	2.7489	(0.0038)	−1.6753	(0.0030)	−0.4838	(−0.0008)

[a] The aug-cc-pVDZ MC$^+$BS basis set with the 3*s*3*p*2*d*2*f* midbond set was used. The errors resulting from density fitting are given in parentheses. The unit for the energies and the errors is kcal/mol. All calculations in double precision.

benefits. The frequency integral in formula 5 for the dispersion energy was evaluated using an 8-point Gauss-Legendre quadrature, and the first two terms were used in expansion 27 of ref 22 (i.e., two iterations were performed in solving the TD-DFT set of equations for the propagator matrix $\tilde{\mathbf{C}}$).

B. Benzene Dimer. The results for the benzene dimer in the parallel ("sandwich") geometry are presented in Table 1. The intermolecular distances were chosen to range from 3.2 Å (repulsion wall), through 3.85 Å (minimum), to 5.0 Å (long-range region). As the table shows, for all the distances the accuracy of density fitting is very satisfactory, the error always being well below 0.01 kcal/mol for all interaction components. For the total interaction energies, the largest discrepancy, 0.018% at the minimum geometry, is much smaller than the error resulting from the incompleteness of the basis set (cf. the results for the dispersion energy with the aug-cc-pVTZ in ref 22). Although the calculation of dispersion energy involves an additional approximation besides density fitting of integrals, namely the truncation of the expansion 27 in ref 22, the error of this component does not dominate the total error, except for the small distances, but even then the error is very small. The relative error is largest for electrostatic term, exceeding 1% for the minimum geometry. This component will be discussed in the next subsection.

C. Accuracy of the Electrostatic Component. As discussed above, the relative errors of density fitting are usually the largest for the electrostatic energy. It is easy to understand why the electrostatic term is difficult to fit. This component, obtained by summing the positive contributions of the electron−electron and nuclear−nuclear repulsion interactions with the negative electron−nuclear attraction term, is typically much smaller in magnitude than either of these three terms. The error introduced by density fitting, which affects only the electron repulsion term, is, in fact, very small, amounting to just 1.4×10^{-6}% of this term for benzene dimer at 3.85 Å. However, this error may still become comparable to the total electrostatic energy, which makes the latter correction particularly sensitive to the quality of the fit.

One way to improve the accuracy of the electrostatic energy is to use larger and/or better auxiliary basis sets. In ref 20, Hesselmann et al. used two different types of auxiliary bases. The so-called JK-optimized bases (named for the symbols denoting the Coulomb and exchange integrals) of ref 51 were used for all SAPT components except for the dispersion and exchange-dispersion energies. For the two latter components, the MP2-optimized bases of ref 49 were applied. The JK auxiliary bases are better suited than the MP2-optimized ones to reproduce products of occupied orbitals requiring large exponents. Thus, in particular the electrostatic and first-order exchange energies may be better fitted by JK bases since these terms depend only on occupied orbitals. Since no JK-basis sets corresponding to the augmented bases of Dunning et al. are available, the authors of ref 20 suggested to use the JK auxiliary bases optimized for the cc-pV(X+1) basis sets, i.e., to increment the cardinal number by one relative to the principal basis set used. When we applied JK basis sets for the benzene dimer, we found that this resulted in some significant numerical instabilities in the electrostatic term. In particular, the results differed by about 0.001 kcal/mol between different computer architectures. It turned out that these problems were not due to the use of the JK-type bases but to the size of the basis sets leading to linear dependencies. For example, the use of the MP2-optimized aug-cc-pVTZ auxiliary basis for the benzene dimer resulted in differences between architectures up to 0.03 kcal/mol (whereas the aug-cc-pVDZ results reported in Table 1 are stable). We have found that the main sources of this numerical error were the inversion of the **J** matrix and the summation of eq 14. By performing these two calculations in quadruple precision, this numerical error can be reduced by several orders of magnitude. We have also tested the singular value decomposition (SVD) method recommended in ref 52 for such cases. With 10^{-7} threshold for neglecting small singular values, the numerical stability was improved, but the overall density-fitting error increased. Therefore, it appears that the use of quadruple precision performs better. Since the inversion of the **J** matrix scales as $O(N^3)$ and is done only once for the whole SAPT(DFT) calculation and the calculation of the **D** matrix of eq 14 for the electrostatic term scales as $O(o^2N_{aux}^2)$, even with quadruple precision both calculations are a small fraction of the total costs. We recommend the quadruple precision approach for auxiliary basis sets larger than about 1400 functions since the numerical precision error becomes larger at this size than the density-fitting error. For all other SAPT(DFT) terms, the numerical instability is below 0.0001 kcal/mol, even for the largest auxiliary basis sets tested, and the quadruple precision is not necessary.

With the quadruple precision procedure, we found that the JK-optimized basis sets give more accurate results for the

Table 2: Decomposition of the SAPT(DFT) Interaction Energy Obtained with Density Fitting for Two Argon Atoms Separated by 3.75 Å[a]

	aug-cc-pVDZ		aug-cc-pVTZ	
$E^{(1)}_{elst}$(KS)	−51.451	(−0.446)	−49.718	(0.364)
$E^{(1)}_{exch}$(KS)	169.504	(0.022)	169.642	(0.002)
$E^{(2)}_{ind}$(CKS)	−66.910	(0.000)	−65.850	(−0.000)
$\tilde{E}^{(2)}_{exch-ind}$(CKS)	65.582	(−0.003)	64.718	(0.000)
$E^{(2)}_{disp}$(CKS)	−222.617	(−1.647)	−229.297	(−0.002)
$\tilde{E}^{(2)}_{exch-disp}$(CKS)	15.735	(−0.089)	16.227	(−0.044)
$E^{SAPT(DFT)}_{int}$	−90.158	(−2.163)	−94.280	(0.319)

[a] The aug-cc-pVDZ and aug-cc-pVTZ DC$^+$BS basis sets with the 3*s*3*p*2*d*2*f* midbond set were used. The errors resulting from density fitting are given in parentheses. The unit for the energies and the errors is cm^{-1}. All calculations in double precision.

electrostatic component than the MP2-optimized auxiliary basis of similar size. For benzene dimer at 3.85 Å and the aug-cc-pVDZ principal basis set, the cc-pVTZ JK auxiliary basis set (N_{aux} = 1408) gives 0.0003 kcal/mol density-fitting error in comparison to the 0.0019 kcal/mol error for the MP2-optimized aug-cc-pVDZ auxiliary basis set (N_{aux} = 1240). For the aug-cc-pVTZ principal basis set, the density-fitting errors are −0.002 kcal/mol and −0.005 kcal/mol for JK-cc-pVTZ and MP2-aug-cc-pVTZ (N_{aux} = 1924) auxiliary bases, respectively. Thus, if a very high accuracy of the electrostatic component is required, we recommend the use of JK-optimized bases for this component. In most cases, however, the MP2-optimized bases should be adequate for all components.

D. Argon Dimer. In Table 2, we present SAPT(DFT) results for the argon dimer at the van der Waals minimum. For the aug-cc-pVDZ case, the largest fitting error is in the dispersion term, and the resulting total energy error is 2.5%. This error is considerably larger than for other examples tested. Thus, the argon auxiliary basis set of ref 49 appears somewhat less accurate than other bases of the same size. Still, the error resulting from density fitting is a few times smaller than the basis set incompleteness error which is about 8% (cf. results in the aug-cc-pVQZ basis in ref 13). Therefore, the aug-cc-pVDZ auxiliary basis is in fact adequate. However, the aug-cc-pVTZ basis set performs much better. The largest fitting error is now in the electrostatic term, and the total energy error is only about 0.3%.

E. Water Dimer. Water dimer has been chosen as an example of a polar system. The results presented in Table 3 show that the accuracy of density-fitting is excellent with the largest percentage error of 0.01% in the exchange-dispersion energy. Although in this case the density-fitting errors are negligible already when the aug-cc-pVDZ basis set is used, the aug-cc-pVTZ basis reduces these errors further, as for the argon dimer. This is a very positive observation since with larger basis sets one aims for higher accuracy. Notice that for the water dimer as well as for the benzene and argon dimers the induction and exchange-induction components always exhibit the highest accuracy, exceeding in most cases the number of significant figures presented in the tables. Apparently, the polarization phenomenon results in smooth, easy to fit densities.

Table 3: Decomposition of the SAPT(DFT) Interaction Energy Obtained with Density Fitting for the Water Dimer in a Geometry Close to the Global Minimum[a]

	aug-cc-pVDZ		aug-cc-pVTZ	
$E^{(1)}_{elst}$(KS)	−6.8900	(0.0014)	−6.8847	(−0.0002)
$E^{(1)}_{exch}$(KS)	5.7418	(0.0027)	5.7399	(0.0003)
$E^{(2)}_{ind}$(CKS)	−2.4185	(0.0007)	−2.5381	(0.0000)
$\tilde{E}^{(2)}_{exch-ind}$(CKS)	1.2461	(−0.0001)	1.3417	(0.0000)
$E^{(2)}_{disp}$(CKS)	−2.0350	(0.0001)	−2.3806	(0.0004)
$\tilde{E}^{(2)}_{exch-disp}$(CKS)	0.3420	(−0.0008)	0.4037	(−0.0005)
$E^{SAPT(DFT)}_{int}$	−4.0136	(0.0040)	−4.3180	(−0.0000)

[a] Geometry as in ref 11 with R = 3 Å. The aug-cc-pVDZ and aug-cc-pVTZ basis sets in the DCBS form were used (without midbond). The errors resulting from density fitting are given in parentheses. The unit for the energies and the errors is kcal/mol. All calculations in double precision.

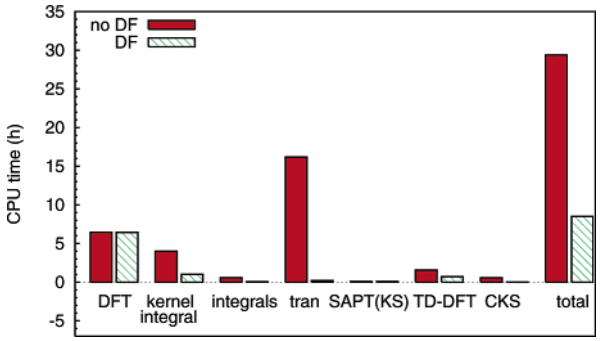

Figure 1. Wall times for the benzene dimer on the 2.4 GHz Opteron processor. The aug-cc-pVDZ basis set with 3*s*3*p*2*d*2*f* midbond was used, corresponding to o = 21, v = 303, N_{aux} = 1240, g = 389 448 grid points in the DFT and TD-DFT calculations. 'DF'—timings with density fitting. 'no DF'—standard DALTON-based SAPT(DFT) with LDA kernel. 'DFT'—two monomer DFT calculations; 'kernel integral'—eq 21 for the DF approach or eq 20 for the no-DF approach for both monomers; 'integrals'—3-index (DF) or 4-index (no-DF) integrals of the dimer; 'tran'—integral transformation; 'SAPT(KS)'—total time for SAPT(KS) terms; 'TD-DFT'——time of computing TD-DFT propagators, 'CKS'—the CKS induction and dispersion energies.

F. Timings of SAPT(DFT). Figure 1 shows the wall-clock times of various steps in the calculations for the benzene dimer, using both the standard and density-fitted SAPT(DFT) approaches. Overall, density fitting accelerates this calculation more than three times with much larger speedups for some of the components. While the major speedup occurs in the transformation step, substantial improvements are also visible in the timings of the calculation of the integrals of eqs 20 and 21 and of the TD-DFT and CKS calculations. For systems such as those treated in this work, the overall timing of the density-fitting approach is now dominated by the monomer Kohn−Sham calculations. This is partly due to the fact that the Kohn−Sham code used by us does not yet take advantage of density fitting (this is also the reason that the overall speedup is only a factor of 3). It is also worth pointing out that a supermolecular DFT calculations for this system would take more time than the SAPT(DFT) calculation (and would produce a worthless result). For larger systems, the benefit of density fitting will show up mostly

Table 4: Decomposition of the SAPT(DFT) Interaction Energy Obtained with Density Fitting for RDX Dimer in a Geometry Extracted from Crystal Structure[53] and Specified in the Supporting Information[54] [a]

$E^{(1)}_{elst}$(KS)	−4.984
$E^{(1)}_{exch}$(KS)	2.867
$E^{(2)}_{ind}$(CKS)	−1.080
$\tilde{E}^{(2)}_{exch-ind}$(CKS)	0.465
$E^{(2)}_{disp}$(CKS)	−3.487
$\tilde{E}^{(2)}_{exch-disp}$(CKS)	0.213
$E^{SAPT(DFT)}_{int}$	−6.006

[a] The cc-pVDZ basis set in the MC+BS form with 3*s*3*p*2*d*2*f* midbond was used. The unit of energy is kcal/mol. All calculations in double precision.

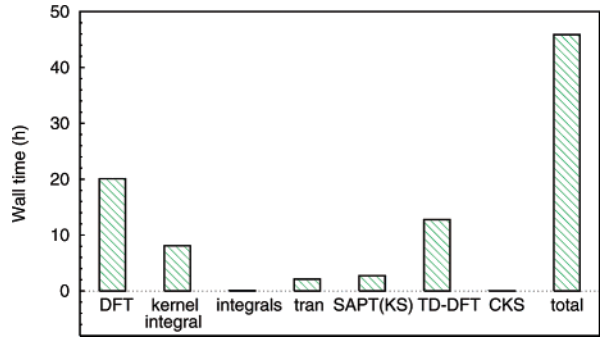

Figure 2. Wall times for the RDX dimer on 2.4 GHz Opteron. The cc-pVDZ basis set with 3*s*3*p*2*d*2*f* midbond was used corresponding to $o = 57$, $v = 366$, $N_{aux} = 1948$, $g = 742\,375$ grid points in the DFT and TD-DFT calculations. For the meaning of the symbols, see Figure 1.

in the CKS steps (TD-DFT matrix multiplications and the dispersion energy evaluation), as the scaling of these steps is reduced from the sixth to the fifth power of system size.

To demonstrate the capabilities of the present approach, we show the results for the RDX dimer in Table 4. Availability of accurate interaction potentials for systems such as RDX is crucial for first-principles predictions of properties of molecular crystals. Due to the size of this system ($o = 57$, $n = 423$), the use of the standard SAPT(DFT) algorithm turned out to be not possible with our current computer resources. Therefore, only the results with density-fitting are shown. Judging from the performance of this approach for other systems, also here the fitting error is most likely negligible and the presented interaction energy components are the most accurate ab initio results to date available for this system. It should be noted that SAPT(DFT) is currently the only practical method of accurately calculating the dispersion energy for systems of the size of RDX. Table 4 shows that, for the considered geometry, the latter component constitutes more than half of the total interaction energy and certainly cannot be neglected in any simulations of the crystal structure.

In Figure 2, the timings of our density-fitted calculations for the RDX dimer are presented. Although the monomer Kohn−Sham portion is still the most time-consuming, the $O(N^5)$ TD-DFT step is now seen to take a comparable amount of time. The cost of transformation, although nominally also scaling as $O(N^5)$, is relatively small due to a smaller prefactor

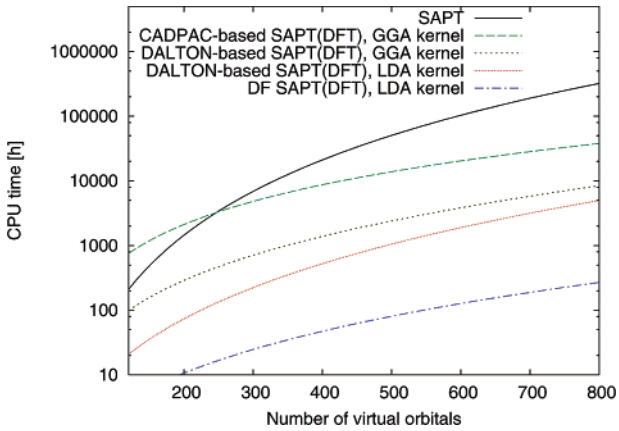

Figure 3. Estimates of the timings for the RDX dimer based on theoretical scaling and extrapolation of the data obtained for smaller systems. 'CADPAC-based SAPT(DFT)' refers to the implementation of ref 10 with no density fitting, 'DALTON-based SAPT(DFT)' is the version without density fitting, 'DF SAPT(DFT)'—density-fitting implementation of the present work and of ref 22, DALTON-based.

than in the case of the TD-DFT terms. Thus, for still larger systems, the latter step is going to dominate the whole calculation.

In Figure 3, we present a visualization of the overall numerical scalings of the SAPT-based methods. We assumed $o = 57$, as for the RDX dimer. The results of the graph were obtained by fitting timings of the various steps of the calculation for the dimethylnitroamine (DMNA) and benzene dimers. Although exact timings cannot be predicted in this way, the graph provides a qualitative comparison of the methods. The regular SAPT calculations are several orders of magnitude more time-consuming than density-fitted SAPT(DFT) ones and significantly more time-consuming than even the CADPAC-based SAPT(DFT) calculations, except for small basis sets where the latter suffer from an inefficient implementation of the integral 20 in CADPAC. Similar conclusions would hold for other correlated methods which include contributions from triple excitations, for example for the coupled cluster method with single, double, and noniterative triple excitations [CCSD(T)]. Our current, DALTON-based implementation is much faster than the former CADPAC-based one of ref 10 mainly due to the more efficient programing of integral 20. The use of the LDA kernel in integral 20 produces another important speedup with a minimal loss of accuracy, as shown in ref 10. Still, the largest relative speedup is due to the use of density fitting implemented in the present work and in ref 22. At the edge of the figure, i.e., for $v = 800$, SAPT calculations (or CCSD(T) calculations) would require 27 years of CPU time, whereas SAPT(DFT) calculations with density fitting take 11 days, a medium-size task if the work is distributed among a few dozen processors.

VI. Conclusions

We have presented a complete implementation of the SAPT(DFT) method based on density fitting of molecular integrals. The density-fitting approximation, applied at the stages of integral transformation, TD-DFT calculations, and in evalu-

ation of the CKS induction and dispersion energies, results in reductions of scaling and operation counts of these most time-consuming steps and hence offers a significant speedup over the standard formulation without density fitting. The overall time requirement of density-fitting SAPT(DFT) scales as $O(N^5)$ in contrast to the $O(N^6)$ scaling of the standard version. Moreover, the memory and IO-requirements of the algorithm are also greatly reduced. All these improvements enable high-accuracy studies of interactions in molecular complexes inaccessible to the standard, wave function-based ab initio methods. The interaction energy for an example of such a complex, the RDX dimer consisting of 42 atoms, 57 occupied orbitals, and using a basis set containing 423 functions, has been computed in this work. Although density-fitting introduces an error in the calculated interaction energies, we have shown that this error is very small, well below 1% for individual energy components. Our implementation is valid for both nonhybrid and hybrid density functionals. As shown in ref 22, in the latter case, an additional (besides density fitting of integrals) approximation has to be applied to bring the cost of obtaining the CKS propagators to $O(N^5)$ scaling. This approximation, consisting in truncation of an iterative scheme of solving the TD-DFT equations, does not significantly impair the overall accuracy.[22] Our new algorithms are flexible with respect to the type of basis sets, i.e., work with both dimer- and monomer-centered bases, including the monomer-centered 'plus' sets of ref 24, which are usually a good compromise between the size of the basis set and accuracy of the computed interaction energies. The implementation utilizes parts of the existing SAPT2002 suite of codes[23] and therefore can readily benefit from developments and updates made in this suite. In particular, the third-order code recently added to SAPT2002 can be used to extend SAPT(DFT). Work in this direction is in progress. The method can also be applied to three-body interactions.[55−57]

Acknowledgment. Funding for this work was provided by an ARO DEPSCOR grant and by the NSF grant CHE0239611.

Supporting Information Available: The RDX dimer geometry. This material is available free of charge via the Internet at http://pubs.acs.org.

References

(1) Jeziorski, B.; Moszynski, R.; Szalewicz, K. *Chem. Rev.* **1994**, *94*, 1887−1930.

(2) Jeziorski, B.; Szalewicz, K. In *Encyclopedia of Computational Chemistry*; von Ragué Schleyer, P., et al., Eds.; Wiley: Chichester, 1998; Vol. 2, pp 1376−1398.

(3) Jeziorski, B.; Szalewicz, K. In *Handbook of Molecular Physics and Quantum Chemistry*; Wilson, S., Ed.; Wiley: 2003; Vol. 3, Part 2, Chapter 9, pp 232−279.

(4) Williams, H. L.; Chabalowski, C. F. *J. Phys. Chem. A* **2001**, *105*, 646−659.

(5) Misquitta, A. J.; Szalewicz, K. *Chem. Phys. Lett.* **2002**, *357*, 301−306.

(6) Hesselmann, A.; Jansen, G. *Chem. Phys. Lett.* **2002**, *357*, 464−470.

(7) Hesselmann, A.; Jansen, G. *Chem. Phys. Lett.* **2002**, *362*, 319−325.

(8) Misquitta, A. J.; Jeziorski, B.; Szalewicz, K. *Phys. Rev. Lett.* **2003**, *91*, 033201.

(9) Hesselmann, A.; Jansen, G. *Chem. Phys. Lett.* **2003**, *367*, 778−784.

(10) Misquitta, A. J.; Podeszwa, R.; Jeziorski, B.; Szalewicz, K. *J. Chem. Phys.* **2005**, *123*, 214103.

(11) Misquitta, A. J.; Szalewicz, K. *J. Chem. Phys.* **2005**, *122*, 214109.

(12) Szalewicz, K.; Podeszwa, R.; Misquitta, A. J.; Jeziorski, B. In *Lecture Series on Computer and Computational Science. ICCMSE 2004*; Simos, T., Maroulis, G., Eds.; VSP: Utrecht, 2004; Vol. 1, pp 1033−1036.

(13) Podeszwa, R.; Szalewicz, K. *Chem. Phys. Lett.* **2005**, *412*, 488−493.

(14) Baerends, E. J.; Ellis, D. E.; Ros, P. *Chem. Phys.* **1973**, *2*, 41−51.

(15) Sambe, H.; Felton, R. *J. Chem. Phys.* **1975**, *62*, 1122−1126.

(16) Dunlap, B. I.; Connolly, J. W. D.; Sabin, J. R. *J. Chem. Phys.* **1979**, *71*, 4993−4999.

(17) Jamorski, C.; Casida, M. E.; Salahub, D. R. *J. Chem. Phys.* **1995**, *104*, 5134−5147.

(18) Dunlap, B. I. *Phys. Chem. Chem. Phys.* **2000**, *2*, 2113−2116.

(19) Werner, H.-J.; Manby, F. R.; Knowles, P. J. *J. Chem. Phys.* **2003**, *118*, 8149−8160.

(20) Hesselmann, A.; Jansen, G.; Schütz, M. *J. Chem. Phys.* **2005**, *122*, 014103.

(21) Della Sala, F.; Görling, A. *J. Chem. Phys.* **2001**, *115*, 5718−5732.

(22) Bukowski, R.; Podeszwa, R.; Szalewicz, K. *Chem. Phys. Lett.* **2005**, *414*, 111−116.

(23) *SAPT2002: An Ab Initio Program for Many-Body Symmetry-Adapted Perturbation Theory Calculations of Intermolecular Interaction Energies*; by Bukowski, R.; Cencek, W.; Jankowski, P.; Jeziorski, B.; Jeziorska, M.; Kucharski, S. A.; Lotrich, V. F.; Misquitta, A. J.; Moszynski, R.; Patkowski, K.; Rybak, S.; Szalewicz, K.; Williams, H. L.; Wormer, P. E. S. University of Delaware and University of Warsaw (http://www.physics.udel.edu/∼szalewic/SAPT/SAPT.html).

(24) Williams, H. L.; Mas, E. M.; Szalewicz, K.; Jeziorski, B. *J. Chem. Phys.* **1995**, *103*, 7374−7391.

(25) Longuet-Higgins, H. C. *Discuss. Faraday Soc.* **1965**, *40*, 7−18.

(26) Zaremba, E.; Kohn, W. *Phys. Rev. B* **1976**, *13*, 2270−2285.

(27) McWeeny, R. *Croat. Chem. Acta* **1984**, *57*, 865−878.

(28) Angyan, J. G.; Jansen, G.; Loos, M.; Hattig, C.; Hess, B. A. *Chem. Phys. Lett.* **1994**, *219*, 267−273.

(29) DALTON, a molecular electronic structure program, Release 2.0 2005, see http://www.kjemi.uio.no/software/dalton/dalton.html.

(30) CADPAC: The Cambridge Analytic Derivatives Package Issue 6, Cambridge, 1995. A suite of quantum chemistry programs developed by R. D. Amos with contributions from I. L. Alberts et al.

(31) Tozer, D. J.; Handy, N. C. *J. Chem. Phys.* **1998**, *109*, 10180−10189.

(32) Tozer, D. J.; Amos, R. D.; Handy, N. C.; Roos, B. O.; Serrano-Andrés, L. *Mol. Phys.* **1999**, *97*, 859−868.

(33) Lee, A. M.; Colwell, S. M. *J. Chem. Phys.* **1994**, *101*, 9704−9709.

(34) Ioannou, A. G.; Colwell, S. M.; Amos, R. D. *Chem. Phys. Lett.* **1997**, *278*, 278−284.

(35) Colwell, S. M.; Handy, N. C.; Lee, A. M. *Phys. Rev. A* **1996**, *53*, 1316−1322.

(36) Colwell, S. M.; Murray, C. W.; Handy, N. C.; Amos, R. D. *Chem. Phys. Lett.* **1993**, *210*, 261−268.

(37) Schmidt, M. W.; Baldridge, K. K.; Boatz, J. A.; Elbert, S. T.; Gordon, M. S.; Jensen, J. H.; Koseki, S.; Matsunaga, K. A. N.; Su, S. J.; Windus, T. L.; Dupuis, M.; Montgomery, J. A. *J. Comput. Chem.* **1993**, *14*, 1347−1363.

(38) Casida, M. E. In *Recent Advances in Density-Functional Theory Part I, Time-Dependent Density Functional Response Theory for Molecules*; Chong, D. P., Ed.; World Scientific: Singapore, 1995; pp 155−192.

(39) Amos, R. D.; Handy, N. C.; Knowles, P. J.; Rice, J. E.; Stone, A. J. *J. Phys. Chem.* **1985**, *89*, 2186−2192.

(40) van Gisbergen, S. J. A.; Snijders, J. G.; Baerends, E. J. *Comput. Phys. Comm.* **1999**, *118*, 119−138.

(41) Jeziorski, B.; Moszynski, R.; Ratkiewicz, A.; Rybak, S.; Szalewicz, K.; Williams, H. L. In *Methods and Techniques in Computational Chemistry: METECC-94*; Clementi, E., Ed.; STEF: Cagliari, 1993; Vol. B, pp 79−129.

(42) Patkowski, K.; Jeziorski, B.; Szalewicz, K. *J. Chem. Phys.*, submitted.

(43) Whaley, R. C.; Petitet, A.; Dongarra, J. J. *Parallel Comput.* **2001**, *27*, 3−35.

(44) Perdew, J. P.; Burke, K.; Ernzerhof, M. *Phys. Rev. Lett.* **1996**, *77*, 3865−3868.

(45) Adamo, C.; Barone, V. *J. Chem. Phys.* **1999**, *110*, 6158−6170.

(46) Fermi, E.; Amaldi, E. *Mem. Accad. Italia* **1934**, *6*, 119−149.

(47) Lias, S. G. Ionization Energy Evaluation, in NIST Chemistry WebBook, NIST Standard Reference Database Number 69 (http://webbook.nist.gov).

(48) Kendall, R. A.; Dunning, T. H.; Harrison, R. J. *J. Chem. Phys.* **1992**, *96*, 6796−6806.

(49) Weigend, F.; Köhn, A.; Hättig, C. *J. Chem. Phys.* **2002**, *116*, 3175−3183.

(50) Tsuzuki, S.; Honda, K.; Mikami, M.; Tanabe, K. *J. Am. Chem. Soc.* **2002**, *124*, 104−112.

(51) Weigend, F. *Phys. Chem. Chem. Phys.* **2002**, *4*, 4285−4291.

(52) Cisneros, G. A.; Piquemal, J.-P.; Darden, T. A. *J. Chem. Phys.* **2005**, *123*, 044109.

(53) Choi, C. S.; Prince, E. *Acta Crystallogr.* **1972**, *B 28*, 2857−2862.

(54) See the Supporting Information.

(55) Lotrich, V. F.; Szalewicz, K. *J. Chem. Phys.* **1997**, *106*, 9668−9702.

(56) Lotrich, V. F.; Szalewicz, K. *Phys. Rev. Lett.* **1997**, *79*, 1301−1304.

(57) Lotrich, V. F.; Szalewicz, K. *J. Chem. Phys.* **2000**, *112*, 112−121.

CT050304H